jmb

Hydroxylation of Compactin (ML-236B) by CYP105D7 (SAV_7469) from *Streptomyces avermitilis* [S]

Qiuping Yao[1†], Li Ma[2†], Ling Liu[1], Haruo Ikeda[3], Shinya Fushinobu[4], Shengying Li[2], and Lian-Hua Xu[1*]

[1]*Ocean College, Zhejiang University, Dinghai, Zhoushan, Zhejiang 316021, P.R. China*

[2]*Key Laboratory of Biofuels, Shandong Provincial Key Laboratory of Synthetic Biology, Qingdao Institute of Bioenergy and Bioprocess Technology, Chinese Academy of Sciences, Qingdao, Shandong 266101, P.R. China*

[3]*Kitasato Institute for Life Sciences, Kitasato University, Kanagawa 252-0373, Japan*

[4]*Department of Biotechnology, Graduate School of Agriculture and Life Sciences, The University of Tokyo, Tokyo 113-8657, Japan*

Compactin and pravastatin are competitive cholesterol biosynthesis inhibitors of 3-hydroxy-3-methylglutaryl-CoA reductase and belong to the statin drugs; however, the latter shows superior pharmacokinetic characteristics. Previously, we reported that the bacterial P450, CYP105D7, from *Streptomyces avermitilis* can catalyze the hydroxylation of 1-deoxypentalenic acid, diclofenac, and naringenin. Here, we demonstrate that CYP105D7 could also catalyze compactin hydroxylation in vitro. In the presence of both bacterial and cyanobacterial redox partner systems with an NADPH regeneration system, the reaction produced two hydroxylated products, including pravastatin (hydroxylated at the C6 position). The steady-state kinetic parameters were measured using the redox partners of putidaredoxin and its reductase. The K_m and k_{cat} values for compactin were 39.1 ± 8.8 μM and 1.12 ± 0.09 min^{-1}, respectively. The k_{cat}/K_m value for compactin (0.029 min^{-1}·μM^{-1}) was lower than that for diclofenac (0.114 min^{-1}·μM^{-1}). Spectroscopic analysis showed that CYP105D7 binds to compactin with a K_d value of 17.5 ± 3.6 μM. Molecular docking analysis was performed to build a possible binding model of compactin. Comparisons of different substrates with CYP105D7 were conclusively illustrated for the first time.

Keywords: Compactin, CYP105D7, pravastatin, *Streptomyces avermitilis*, hydroxylation

Introduction

Cytochrome P450s (CYP or P450) are a superfamily of heme-thiolate proteins found in archaea, bacteria, and eukaryotes [1, 2]. P450s catalyze an enormous variety of natural products, such as macrolides, polyenes, glycopeptides, alkaloids, fatty acids, and aromatic polyketides, with oxidative reactions involving regio- and stereospecific hydroxylation, epoxidation, dealkylation, and dehalogenation [3, 4]. With a high specific capacity, the majority of versatile P450 biocatalysts have been gradually used in the pharmaceutical industry [5]. Microbial P450s are attracting more attention as new sources of biocatalysts, because of their important biomedical and environmental roles. Recent efforts for developing the usage of microbial P450s

involve protein engineering, substrate engineering, guest/host activation, and functional screening strategies [6]. Furthermore, microbial P450s are more amenable to functional characterization and X-ray structure analysis [3].

The CYP105 family is associated with a wide range of xenobiotic degradation and antibiotic synthesis, and has at least 17 subfamilies represented in Streptomycetes [7, 8]. In particular, the CYP105D subfamily has been characterized from structural and functional aspects in recent years. CYP105D1 from *Streptomyces griseus* [9], CYP105D5 from *Streptomyces coelicolor* [10], and CYP105D6 from *Streptomyces avermitilis* [11] are prominent examples. Recently, we have reported that CYP105D7 from *S. avermitilis* not only hydroxylates 1-deoxypentalenic acid at the C1 position [12], but also catalyzes the hydroxylation of diclofenac at

the C4′ position [13] and the hydroxylation of naringenin at the 3′ position [14], using the redox partners putidaredoxin (Pdx) and putidaredoxin reductase (Pdr) from *Pseudomonas putida*. Furthermore, an innovative cyanobacterial redox system composed of *se*Fdx (SynPcc7942_1499) and *se*FdR (SynPcc7942_0978) from *Synechococcus elongates* PCC 7942 has been reported in a biofuel study [15] and applied in our study.

Compactin (ML-236B), which was originally isolated from *Penicillium citrinum*, can competitively inhibit the rate-limiting enzyme 3-hydroxy-3-methylglutaryl-CoA reductase in cholesterol biosynthesis [16]. Pravastatin (compactin hydroxylated at position C6), which can effectively reduce the level of low-density lipoprotein in the plasma, can lower the risk of hypercholesterolemia owing to superior pharmacokinetic characteristics [17]. In industry, compactin is converted to pravastatin using *Streptomyces carbophilus*. In fact, P450sca (CYP105A3) from this bacterium has been reported to catalyze this reaction [18]. Recently, a new cytochrome P450 (CYP105AS1) from *Amycolatopsis orientalis* has been reported to catalyze the terminal hydroxylation step of compactin [19].

Here, we demonstrated that CYP105D7 catalyzed the hydroxylation of position C6 of compactin in vitro in the presence of the redox partners Pdx/Pdr, to obtain the valuable drug pravastatin (Fig. 1), in addition to another hydroxylation product. The ligand binding affinity and catalytic activity were measured by spectroscopic and steady-state kinetic analyses. Molecular docking analysis was performed to build a possible binding model of compactin to CYP105D7.

Materials and Methods

Materials

The lactone form of compactin and an authentic sample of pravastatin sodium were obtained from Aladdin (China). Diclofenac sodium and 4′-hydroxydiclofenac were purchased from Sigma-Aldrich (USA). Antibiotics and NADPH were purchased from

Solarbio (China). Enzymes were purified by Ni-nitrilotriacetic acid (NTA) resin (Qiagen, USA), Amicon ultracentrifugal filters (Millipore, USA), and a PD-10 desalting column (GE Healthcare, USA). All other chemicals were of the highest grade.

Expression and Purification of CYP105D7, Redox Partners and GDH

CYP105D7 protein with a 4-His tag at the C-terminus was expressed as described previously [12]. For the expression of Pdx, Pdr, *se*Fdx, *se*FdR, and glucose dehydrogenase (GDH) from *Bacillus subtilis*, *Escherichia coli* BL21(DE3) cells harboring the vectors pET28b-*pdx*, pET19b-*pdr* (with NdeI and BamHI restriction enzyme cleavage sites), pET28b-*sefdx*, pET28b-*sefdR*, and pET28b-*gdh*, respectively, were cultured overnight at 37°C in Luria-Bertani (LB) medium containing 50 μg/ml of kanamycin (100 μg/ml ampicillin and 50 μg/ml kanamycin for pET19b-*pdr*). Then, the overnight culture was inoculated into 1 L of LB medium (1:100) containing 50 μg/ml kanamycin, or 100 μg/ml ampicillin and 50 μg/ml kanamycin, 5% glycerol, and rare salt solution at 37°C. Cells were cultured for 3–4 h until the OD_{600} reached 0.6–1.0. Next, isopropyl β-D-thiogalactopyranoside (0.2 mM) was added to induce protein expression, and the cells were cultured at 18°C for 20–24 h.

For protein purification, the cell pellet was resuspended in lysis buffer (50 mM NaH_2PO_4, 300 mM NaCl, 10% glycerol, and 10 mM imidazole, pH 8.0) and vortexed. A Model 500 Sonic Dismembrator (Scientz, China) was used for sonication. The soluble fraction was collected by centrifugation at 10,000 ×*g* for 60 min at 4°C, and then incubated at 4°C for 1–2 h after adding (usually 1–2 ml per liter of protein) Ni-NTA resin. The slurry was loaded into an empty column, which was washed with one column volume wash buffer (50 mM NaH_2PO_4, 300 mM NaCl, 10% glycerol, and 20 mM imidazole, pH 8.0), and then the protein was washed until impure proteins were eluted in the flow-through. Elution buffer (50 mM NaH_2PO_4, 300 mM NaCl, 10% glycerol, and 250 mM imidazole, pH 8.0) was used to elute the protein fraction, which was concentrated by Amicon ultracentrifugal filters at 6,000 ×*g* for 30 min at 4°C. Finally, the collected fraction was loaded into a PD-10 desalting column pre-equilibrated with 25 ml of desalting buffer containing 50 mM NaH_2PO_4 and 10% glycerol, pH 7.4, and desalting buffer was added for buffer exchange. Protein aliquots were stored at − 80°C after flash freezing with liquid N_2. The
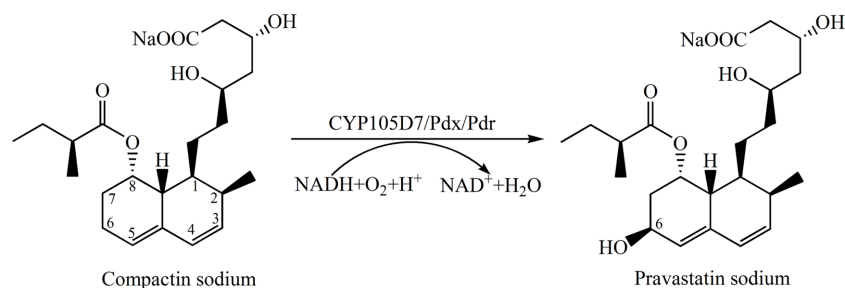

Fig. 1. Schematic representation of the hydroxylation of compactin by CYP105D7.

concentration of CYP105D7 was determined by CO difference spectroscopy [14]. The concentrations of Pdx and *se*Fdx were measured by a Cary 50 Bio spectrophotometer (Varian, USA) using 75 mM ascorbic acid, 10 mM ferrozine, and saturated ammonium acetate at 562 nm. The concentrations of Pdr and *se*FdR were determined using 0.5 mM horse heart cytochrome *c* (in

10 mM potassium phosphate buffer, pH 7.7) and 10 mM NADPH at 550 nm in the kinetic mode on a DU 800 spectrophotometer (Beckman Coulter, USA).

Preparation of Compactin
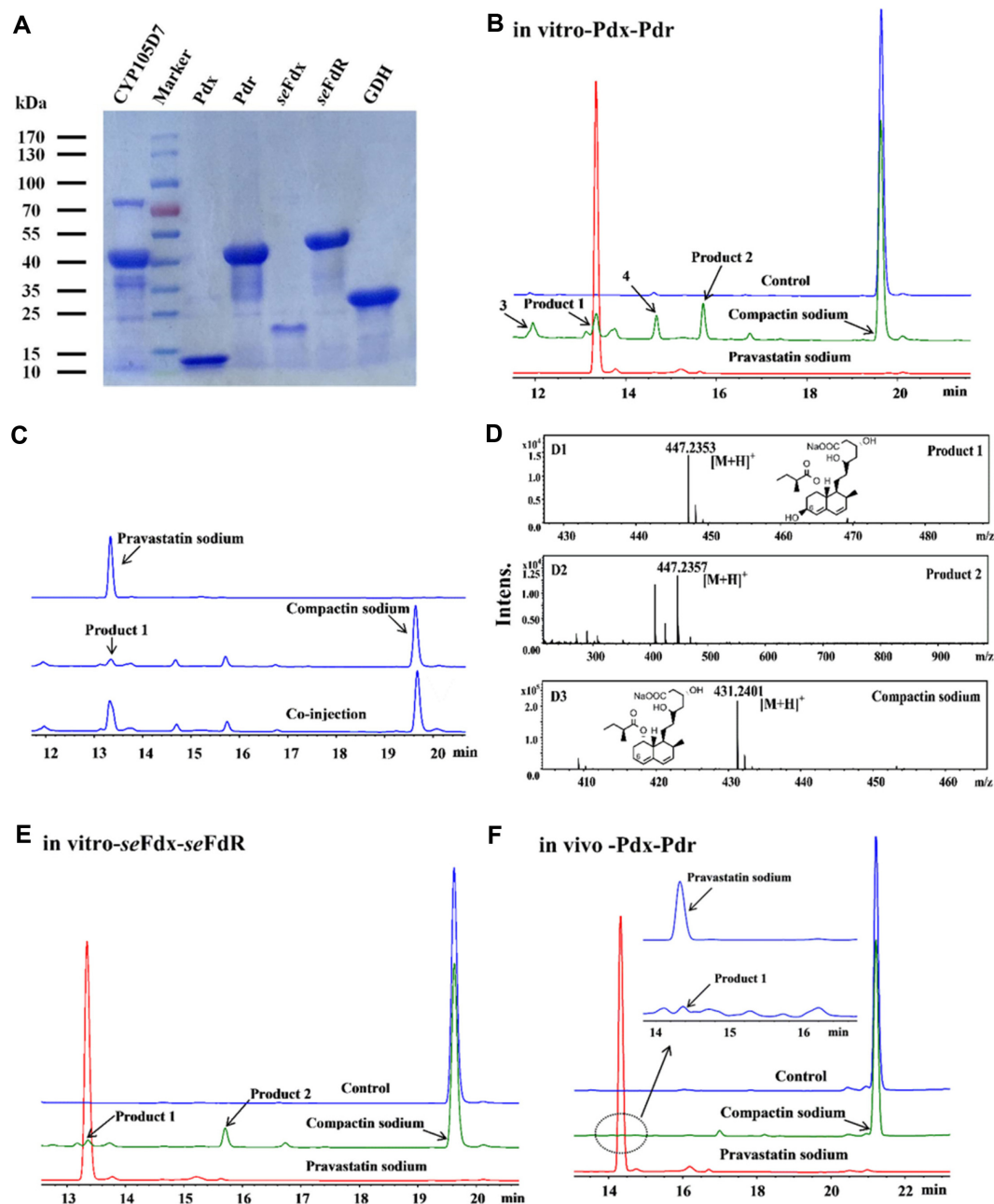
Compactin sodium was prepared by saponification of the

Fig. 2. In vitro and in vivo conversion of compactin by CYP105D7.
(**A**) SDS-PAGE analysis of purified proteins. HPLC analysis of compactin in vitro by CYP105D7 in the presence of the redox partners Pdx/Pdr (**B**) or *se*Fdx/*se*FdR (**E**). (**C**) Comparison of authentic pravastatin sodium, product 1, and co-injection experiment. (**D**) HR-ESI-MS analysis of in vitro activity of CYP105D7 with Pdx/Pdr. (**E**, **F**) HPLC of the bioconversion of compactin using a recombinant CYP105D7-Pdx/Pdr co-expression system with a 12-h incubation. For all HPLC results, the blue, green, and red lines indicate negative control, in vitro or in vivo reaction, and the authentic sample of pravastatin.

lactone form in 96% ethanol-water and 0.1 M NaOH at 50°C for 2 h with stirring. After cooling, 0.1 M HCl was used to adjust the pH value to 7.0. The obtained compound was verified by LC-ESI-MS (Fig. 2D3).

Spectral Substrate Binding Assay

Ultraviolet (UV)-visible absorption spectra and titration experiments were carried out according to a previously developed method [14] using a double-beam spectrophotometer (UV-2101PC; Shimadzu, Japan). The final concentrations of compactin sodium used in the titration experiments were 0, 2, 4, 6, 8, 10, 12, and 16 μM. The K_d was determined by nonlinear fitting with a quadratic equation using Kaleidagraph (Synergy, USA):

$\Delta A = (B_{max}/2E)\{(K_d + E + L) - \{(K_d + E + L)^2 - 4EL\}^{1/2}\}$, where B_{max} is the maximum absorbance difference extrapolated to infinite ligand enzyme concentration, ΔA is the difference in absorbance, E is the total enzyme concentration, L is the ligand concentration, and K_d is the dissociation constant.

In Vitro Bioconversion

The standard reaction mixture contained 20 μM CYP105D7, 20 μM Pdx (or seFdx), 80 μM Pdr (or seFdR), 200 μM compactin (20 mM stock solution was dissolved in methanol), and 1 mM NADPH in 100 μl of desalting buffer. Five units of GDH and 10 mM glucose were added as an NADPH regeneration system. The reaction was initiated by adding 1 mM NADPH at 30°C for 12 h. Then, 100 μl of methanol was added to stop the reaction, the mixture was shaken for 2 min, and the supernatant was collected by centrifugation at 14,000 rpm for 10 min to remove precipitated proteins. The supernatants were analyzed by reverse-phase high-performance liquid chromatography with an Agilent 1260 spectrometer, using a Thermo Scientific Hypersil ODS C_{18} column (4.6 × 150 mm; 5 μm) with a linear gradient system of 20–80% acetonitrile and 0.1% trifluoroacetic acid for 35 min. The flow rate was 1.0 ml/min, detection was at 238 nm, and the injection volume was 40 μl. High-resolution electrospray mass spectrometry (HR-ESI-MS) was recorded by a Dionex Ultimate 3000 connected to a Bruker Maxis Q-TOF under the same elution conditions as HPLC.

In Vivo Bioconversion

We carried out the whole-cell reaction of compactin sodium using *E. coli* transformed with *sav7469* (CYP105D7), *camA* (Pdx), and *camB* (Pdr). The bioconversion was conducted according to a previously developed measurement [14], and the detection conditions were the same as the in vitro measurements.

Molecular Docking Analysis

AutoDock Vina [8] was used to calculate the molecular docking, and the crystal structure of CYP105D7 in complex with diclofenac (PDB ID 4UBS) was used for the docking after removing the ligand [13]. The grid box was centered at the center of the compactin binding site. The size of the grid box was 22.5 Å × 22.5 Å × 22.5 Å, with a 1 Å spacing, covering the whole ligand

molecule. The value of exhaustiveness was set to 8. The other parameters used were the default values.

Steady-State Kinetics

For kinetic measurements, assays were carried out under the above-described HPLC conditions. The reaction contained 5 μM CYP105D7, 5 μM Pdx, 20 μM Pdr, and 20–150 μM compactin sodium in 100 μl of desalting buffer; for diclofenac, the corresponding concentrations were 2, 2, 8, and 20–150 μM. After pre-incubation at 30°C for 5 min in a K30 dry bath incubator (Allsheng, China), the reactions were initiated by adding 1 μl of 100 mM NADPH. The reactions were stopped by adding the equivalent volume of methanol and thorough mixing for 5, 10, 20, 30, 40, 50, and 60 min, respectively. By directly measuring the substrate consumption through HPLC, the initial velocity was deduced from the decreased area under the curve of certain substrate peaks. The steady-state kinetic parameters K_m and k_{cat} were calculated by fitting the data (performed in duplicates) to the Michaelis-Menten equation by nonlinear regression of a hyperbolic function using the OriginPro 8.5 software (OriginLab, USA).

Results

Expression of *S. avermitilis* CYP105D7, Pdx/Pdr, seFdx/seFdR, and GDH in *E. coli*

CYP105D7 with a 4-His tag at the C-terminus was purified to homogeneity (Fig. 2A). The single band of CYP105D7 on the sodium dodecyl sulfate-polyacrylamide gel was at the molecular mass of 45 kDa. The UV-visible absorption spectra of purified CYP105D7 in the ferric (resting), dithionite-reduced, and dithionite-reduced plus CO states have been described previously [12]. The redox partner proteins Pdx/Pdr, seFdx/seFdR, and GDH were expressed and purified to single bands corresponding to 12, 46, 20, 50, and 30 kDa, respectively (Fig. 2A).

In Vitro Conversion of Compactin by CYP105D7

The hydroxylation activity of P450s generally consists of many steps associated with redox partners, which transfer electrons from NAD(P)H to the heme active center [20]. Different redox partners may have different catalytic effects on the P450 reactions [21]. Here, we used two redox partner systems, Pdx/Pdr and seFdx/seFdR, in vitro.

HPLC analysis showed that compactin was hydroxylated by CYP105D7, producing two products (product 1 and product 2) in the presence of the redox partner Pdx/Pdr (Fig. 2B). The retention time of product 1 was 13.351 min, which was identical to that of the authentic pravastatin sample. When we co-injected the mixture of the reaction
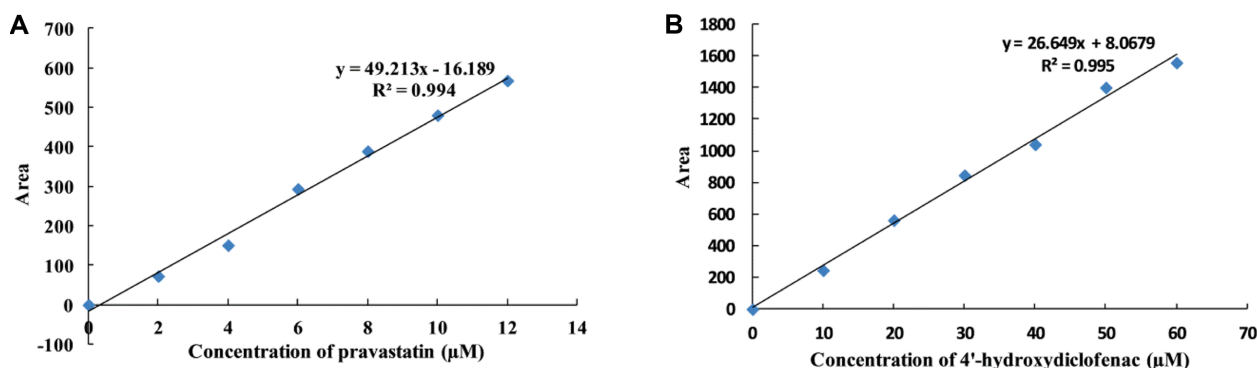
Fig. 3. Standard curve of pravastatin (**A**) and 4'-hydroxydiclofenac (**B**).

product and the authentic pravastatin sodium sample, they eluted in the same peak in HPLC (Fig. 2C). These reactions and detections were carried out in duplicates, and we obtained identical retention times for both product 1 and the authentic pravastatin. HR-ESI-MS was used to further analyze product 1 and compactin. These samples showed m/z values of 447.2353 [M+H]$^+$ (calc. 447.2353 for $C_{23}H_{36}O_7Na$) and 431.2401 [M+H]$^+$ (calc. 431.2404 for $C_{23}H_{36}O_6Na$), respectively (Fig. 2D1, D3). These results demonstrated that CYP105D7 catalyzed compactin at the C6 position to produce pravastatin. HPLC analysis also showed another peak (product 2 with a retention time of 15.711 min). Product 2 showed almost the same UV absorption spectrum as that of compactin, and HR-ESI-MS analysis showed that it has a molecular mass of an m/z value of 447.2357 [M+H]$^+$ (calc. 447.2353 for $C_{23}H_{36}O_7Na$; Fig. 2D2), suggesting that it was another hydroxylated compactin in a different hydroxylation position. The HPLC results showed two additional peaks with retention times of 11.948 min (product 3) and 14.680 min (product 4). These compounds could not be identified, because of their poor degree of ionization by LC-ESI-MS. Thus, we concluded that the redox partner Pdx/Pdr was able to support CYP105D7 to catalyze compactin in an enzymatic bioconversion. The conversion rate of product 1 was quantitatively calculated as 6.3% according to the standard curve (Fig. 3A). However, the conversion rate of product 2 was difficult to calculate. With the other redox partner system, *se*Fdx/*se*FdR, the two hydroxylation products (products 1 and 2) were also obtained, but product 1 showed a lower conversion rate (1.8%) than that of the reaction using Pdx/Pdr (Fig. 2E).

In Vivo Conversion of Compactin by CYP105D7

We examined the conversion of compactin using a co-expression system of the bacterial redox partners Pdx and Pdr for a whole-cell bioconversion reaction in *E. coli.* HPLC analysis revealed that compactin was hydroxylated by CYP105D7. The retention time of the product of compactin sodium (14.37 min) was identical to that of the authentic pravastatin (Fig. 2F), and 1.1% of compactin sodium was converted to the 6-hydroxylated product. This is in accordance with the report that P450sca-2 from *Streptomyces carbophilus* can convert compactin to pravastatin [22]. Other bacterial strains, including *Streptomyces*, *Actinomadura*, and *Pseudonocardia*, have been also shown to have the same bioconversion ability [23–26].

Spectral Characterization

The spectral titration results of CYP105D7 with compactin are shown in Figs. 4A and 4B. The spectral changes of CYP105D7 illustrated a typical type I shift of the Soret peak from low spin (417 nm) to high spin (385 nm). The K_d value for CYP105D7 was estimated to be 17.5 ± 3.6 μM. Furthermore, we used the lactone form of compactin as the substrate in the titration experiment, and the K_d was calculated as 15.3 ± 1.5 μM (data not shown). Therefore, the two different forms (open or closed lactone ring) of compactin show similar binding affinities to CYP105D7.

Molecular Docking of Compactin to CYP105D7

Docking calculations were conducted to further study the ligand binding of CYP105D7 (Fig. 5A). The bound compactin is directly hydrogen bonded with Thr79, Arg81, Leu178, Thr391, and Ile392. The C6 position of compactin is proximate to the heme group, and the distance to the heme iron is 4.8 Å (Fig. 5B), which appears to be appropriate for the 6-hydroxylation reaction. In the case of CYP105D7 and CYP2C5 complexed with diclofenac, the distances between the initial hydroxylation position (C3' or atom) and the
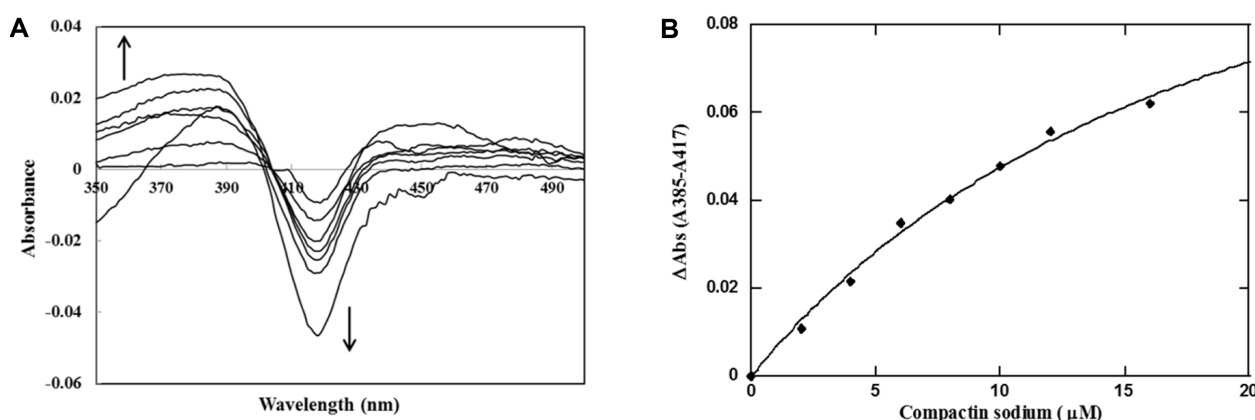
Fig. 4. Spectral changes of CYP105D7 (ferric resting state) upon addition of increasing concentrations of compactin.
(**A**) Difference spectra. (**B**) Titration curve calculated using values of absorption differences at 385 and 417 nm.

heme iron are within a range of 4.4–4.9 Å [13, 27].

Steady-State Kinetic Parameters of CYP105D7 Substrates

The apparent steady-state kinetic parameters were determined by directly monitoring the consumption of substrates using HPLC with the electron-transport redox partners Pdx and Pdr. The K_m and k_{cat} values for compactin were 39.1 ± 8.8 μM and 1.12 ± 0.09 min^{-1}, respectively (Fig. 6A). The catalytic efficiency (k_{cat}/K_m) for compactin was 0.029 min^{-1}·μM^{-1}. For comparison, we also measured the kinetic parameters of the enzymatic conversion of diclofenac by CYP105D7 [13] using this system. The K_m, k_{cat}, and k_{cat}/K_m values for diclofenac were 190 ± 62 μM, 21.6 ± 4.7 min^{-1}, and 0.114 min^{-1}·μM^{-1}, respectively (Fig. 6B). The

conversion rate of diclofenac was approximately 35.8% (Fig. 3B and Fig. S1). We also tried to determine the kinetic parameters of the reaction for naringenin [14], but failed because of a low conversion rate (data not shown).

Discussion

The molecular docking analysis showed that the distal pocket of CYP105D7 binds a single compactin molecule, in contrast to diclofenac and naringenin, which bind two molecules in the pocket [13, 14]. Recently, the crystal structure of the optimized mutant of CYP105AS1 from *A. orientalis* (P450$_{Prava}$) in complex with compactin was reported (PDB code 4OQR) [19]. CYP105D7 and CYP105AS1
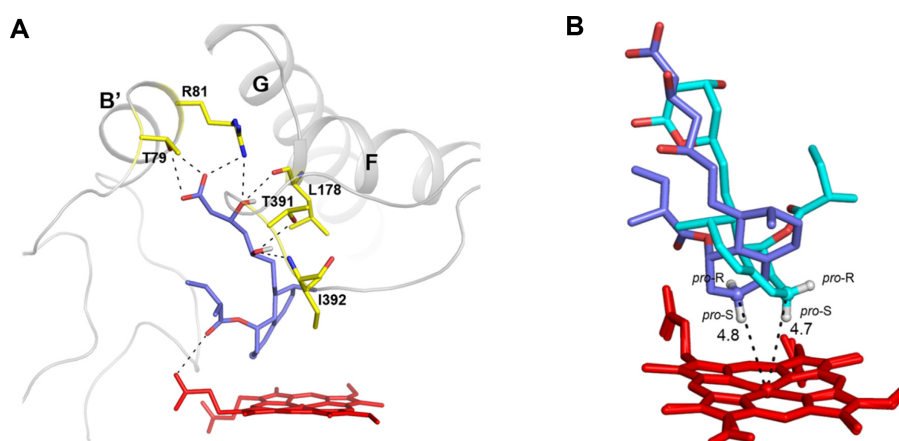

Fig. 5. Docking model of compactin as a substrate for the active site of CYP105D7.
(**A**) Compactin (opened lactone ring), heme, and amino acids are shown as purple, red, and yellow sticks, respectively. Hydrogen bonds are shown as dotted lines. (**B**) Superposition with the crystal structure of the optimized mutant P450$_{Prava}$ of CYP105AS1 from *Amycolatopsis orientalis* in complex with compactin (closed lactone ring, cyan sticks). Hydroxylation positions in compactin are denoted by spheres. *pro*-S and *pro*-R hydrogens are shown as white sticks.
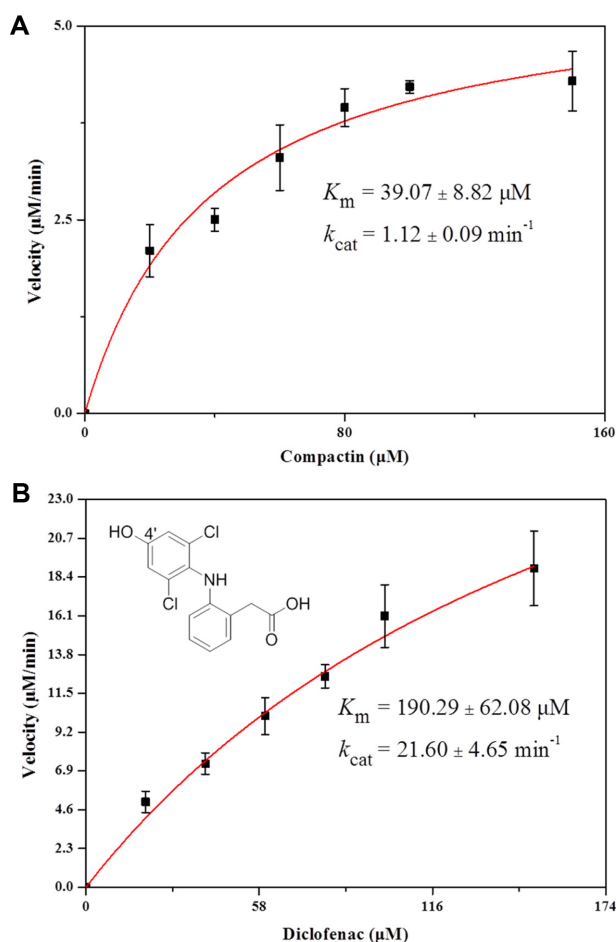
Fig. 6. Michaelis-Menten analysis of CYP105D7 using compactin (**A**) or diclofenac (**B**) as a substrate.

show 44% amino acid sequence identity. A structural similarity search using the Pairwise DALI (Hasegawa and Holm 2009) suggested that CYP105D7 is similar to the structure of CYP105AS1 (RMSD for 376 Cα atoms = 1.8 Å). The superimposition of the docked structure of CYP105D7/compactin with the crystal structure of P450$_{prava}$/compactin (closed form) is shown in Fig. 5B. The hydroxylation position of compactin (C6 atom) in the two P450 structures was located closely, and the distance between the carbon atom at the hydroxylation site and the heme iron was 4.8 (CYP105D7) and 4.7 Å (P450$_{Prava}$), respectively. Furthermore, similar to the P450$_{Prava}$/compactin structure, the *pro*-S hydrogen from the C6 carbon in the CYP105D7/compactin structure points to the heme iron, indicating that the product is not 6-*epi*-pravastatin, but pravastatin. One of the most successful industrial applications of CYP105 biocatalysis for producing pravastatin is CYP105A3 (P450sca-2) [28, 29], but its crystal structure has not yet been reported.

CYP105D7 and CYP105A3 share relatively high amino acid sequence identity (57%), even though they do not belong to the same subfamily. Interestingly, the amino acids involved in the binding of compactin to CYP105D7 (Arg81, Leu178, Thr391, and Ile392) are conserved in CYP105A3, suggesting that these amino acids play a significant role in the binding of compactin with CYP105A3.

To date, CYP105D7 has been reported to hydroxylate daidzein (isoflavone) [30], 1-deoxypentalenic acid [12], diclofenac (nonsteroidal) [13], and naringenin (flavanone) [14] (Fig. S2). Here, we showed that it also hydroxylates compactin, emphasizing the versatility of this enzyme. We also compared the conversion rate and the kinetic parameters of compactin and diclofenac using purified CYP105D7 and the Pdx/Pdr system. The conversion rate of compactin by CYP105D7 in vitro, being about 5-fold lower than that of diclofenac (35.8%), is almost 6-fold higher than that in vivo. The catalytic efficiency (k_{cat}/K_m) of diclofenac was 0.114 min^{-1}·μM^{-1}, which is about 4-fold higher than that of compactin, mainly due to the difference in the k_{cat} values. These results suggest that diclofenac is a more effective substrate than compactin. Moreover, spectral titration and docking analysis results show that compactin binds to the CYP105D7 with one molecular binding mode. This is different from diclofenac and naringenin, which have a multiple-ligand binding mode. CYP105D7 accepts various categories of substrates with different binding modes, similar to the drug metabolizing P450s in humans. Such capacity is ascribed to structural flexibility [10, 12].

To comparatively test the electron transfer efficiency, we used the two redox partner systems Pdx/Pdr and *se*Fdx/*se*FdR. The in vitro conversion results showed that Pdx/Pdr exhibited a nearly 4-fold higher conversion rate than *se*Fdx/*se*FdR. This result emphasizes the significance of selecting suitable redox partners for enhancing the bioconversion efficiency. Several reports have demonstrated that protein-protein interactions with redox partners play a considerable role in modulating the catalytic activity of P450 enzymes, especially for the P450 reductase domain of a self-sufficient P450 from *Rhodococcus* sp. [31, 32].

Because of the higher solubility and easy operation of bacterial P450s, CYP105D7 has potential for industrial application. The k_{cat} values of most P450s range from 1 to 300 min^{-1} [33]. Although the k_{cat} value of the CYP105D7-catalyzed hydroxylation of compactin sodium is in the appropriate range, optimization of the conversion system by directed evolution and/or rational design is necessary. Thus, our future studies will explore biotechnological applications of CYP105D7, to extend the industrial roles to

which it can be applied, and hence more engineering work should be performed.

References

1. Xu LH, Fushinobu S, Ikeda H, Wakagi T, Shoun H. 2009. Crystal structures of cytochrome P450 105P1 from *Streptomyces avermitilis*: conformational flexibility and histidine ligation state. *J. Bacteriol.* **191:** 1211-1219.

2. Makino T, Katsuyama Y, Otomatsu T, Misawa N, Ohnishi Y. 2014. Regio- and stereospecific hydroxylation of various steroids at the 16α position of the D ring by the *Streptomyces griseus* cytochrome P450 CYP154C3. *Appl. Environ. Microbiol.* **80:** 1371-1379.

3. Podust LM, Sherman DH. 2012. Diversity of P450 enzymes in the biosynthesis of natural products. *Nat. Prod. Rep.* **29:** 1251-1266.

4. Bernhardt R. 2006. Cytochromes P450 as versatile biocatalysts. *J. Biotechnol.* **124:** 128-145.

5. Ma L, Du L, Chen H, Sun Y, Huang S, Zheng X, *et al.* 2015. Reconstitution of the in vitro activity of the cyclosporine-specific P450 hydroxylase from *Sebekia benihana* and development of a heterologous whole-cell biotransformation system. *Appl. Environ. Microbiol.* **81:** 6268-6275.

6. Fasan R. 2012. Tuning P450 enzymes as oxidation catalysts. *ACS Catal.* **2:** 647-666.

7. Kelly SL, Kelly DE, Jackson CJ, Warrilow AG, Lamb DC. 2005. The diversity and importance of microbial cytochromes P450, pp. 585-617. *In* Ortiz de Montellano PR (ed.). *Cytochrome P450: Structure, Mechanism, and Biochemistry*, 3rd Ed. Kluwer Academic/Plenum Publishers, New York. USA.

8. Moody SC, Loveridge EJ. 2014. CYP105 — diverse structures, functions and roles in an intriguing family of enzymes in *Streptomyces. J. Appl. Microbiol.* **117:** 1549-1563.

9. Taylor M, Lamb DC, Cannell R, Dawson M, Kelly SL. 1999. Cytochrome P450105D1 (CYP105D1) from *Streptomyces griseus*: heterologous expression, activity, and activation effects of multiple xenobiotics. *Biochem. Biophys. Res. Commun.* **263:** 838-842.

10. Chun Y-J, Shimada T, Sanchez-Ponce R, Martin MV, Lei L, Zhao B, *et al.* 2007. Electron transport pathway for a *Streptomyces* cytochrome P450: cytochrome P450 105D5-catalyzed fatty acid hydroxylation in *Streptomyces coelicolor* A3(2). *J. Biol. Chem.* **282:** 17486-17500.

11. Xu L-H, Fushinobu S, Takamatsu S, Wakagi T, Ikeda H, Shoun H. 2010. Regio- and stereospecificity of filipin hydroxylation sites revealed by crystal structures of cytochrome P450 105P1 and 105D6 from *Streptomyces avermitilis*. *J. Biol. Chem.* **285:** 16844-16853.

12. Takamatsu S, Xu L-H, Fushinobu S, Shoun H, Komatsu M, Cane DE, *et al.* 2011. Pentalenic acid is a shunt metabolite in the biosynthesis of the pentalenolactone family of metabolites: hydroxylation of 1-deoxypentalenic acid mediated by CYP105D7 (SAV_7469) of *Streptomyces avermitilis*. *J. Antibiot.* **64:** 65-71.

13. Xu L-H, Ikeda H, Liu L, Arakawa T, Wakagi T, Shoun H, Fushinobu S. 2015. Structural basis for the 4′-hydroxylation of diclofenac by a microbial cytochrome P450 monooxygenase. *Appl. Microbiol. Biotechnol.* **99:** 3081-3091.

14. Liu L, Yao Q, Ma Z, Ikeda H, Fushinobu S, Xu L-H. 2016. Hydroxylation of flavanones by cytochrome P450 105D7 from *Streptomyces avermitilis*. *J. Mol. Catal. B Enzym.* **132:** 91-97.

15. Zhang J, Lu X, Li J-J. 2013. Conversion of fatty aldehydes into alk(a/e)nes by in vitro reconstituted cyanobacterial aldehyde-deformylating oxygenase with the cognate electron transfer system. *Biotechnol. Biofuels.* **6:** 1.

16. Endo A, Kuroda M, Tsujita Y. 1976. ML-236A, ML-236B, and ML-236C, new inhibitors of cholesterogenesis produced by *Penicillium citrinum. J. Antibiot.* **29:** 1346-1348.

17. Serizawa N. 1996. Biochemical and molecular approaches for production of pravastatin, a potent cholesterol-lowering drug. *Biotechnol. Annu. Rev.* **2:** 373-389.

18. Matsuoka T, Miyakoshi S, Tanzawa K, Nakahara K, Hosobuchi M, Serizawa N. 1989. Purification and characterization of cytochrome P-450sca from *Streptomyces carbophilus*. *Eur. J. Biochem.* **184:** 707-713.

19. McLean KJ, Hans M, Meijrink B, van Scheppingen WB, Vollebregt A, Tee KL, *et al.* 2015. Single-step fermentative production of the cholesterol-lowering drug pravastatin via reprogramming of *Penicillium chrysogenum. Proc. Natl. Acad. Sci. USA* **112:** 2847-2852.

20. Urlacher VB, Girhard M. 2012. Cytochrome P450 monooxygenases: an update on perspectives for synthetic application. *Trends Biotechnol.* **30:** 26-36.

21. Guengerich FP. 2002. Rate-limiting steps in cytochrome P450 catalysis. *Biol. Chem.* **383:** 1553-1564.

22. Watanabe I, Nara F, Serizawa N. 1995. Cloning, characterization and expression of the gene encoding cytochrome P-450sca-in2 from *Streptomyces carbophilus* involved in production of pravastatin, a specific HMG-CoA reductase inhibitor. *Gene* **163:** 81-85.

23. Park J-W, Lee J-K, Kwon T-J, Yi D-H, Kim Y-J, Moon S-H, *et al.* 2003. Bioconversion of compactin into pravastatin by *Streptomyces* sp. *Biotechnol. Lett.* **25:** 1827-1831.

24. Peng Y, Demain AL. 2000. Bioconversion of compactin to

pravastatin by *Actinomadura* sp. ATCC 55678. *J. Mol. Catal. B Enzym.* **10:** 151-156.

25. Chen C-H, Hu H-Y, Cho Y-C, Hsu W-H. 2006. Screening of compactin-resistant microorganisms capable of converting compactin to pravastatin. *Curr. Microbiol.* **53:** 108-112.

26. Fujii Y, Norihisa K, Fujii T, Aritoku Y, Kagawa Y, Sallam KI, *et al.* 2011. Construction of a novel expression vector in *Pseudonocardia autotrophica* and its application to efficient biotransformation of compactin to pravastatin, a specific HMG-CoA reductase inhibitor. *Biochem. Biophys. Res. Commun.* **404:** 511-516.

27. Wester MR, Johnson EF, Marques-Soares C, Dijols S, Dansette PM, Mansuy D, Stout CD. 2003. Structure of mammalian cytochrome P450 2C5 complexed with diclofenac at 2.1Å resolution: evidence for an induced fit model of substrate binding. *Biochemistry* **42:** 9335-9345.

28. Ba L, Li P, Zhang H, Duan Y, Lin Z. 2013. Engineering of a hybrid biotransformation system for cytochrome P450sca-2 in *Escherichia coli*. *Biotechnol. J.* **8:** 785-793.

29. Ba L, Li P, Zhang H, Duan Y, Lin Z. 2013. Semi-rational engineering of cytochrome P450sca-2 in a hybrid system for enhanced catalytic activity: insights into the important role of electron transfer. *Biotechnol. Bioeng.* **110:** 2815-2825.

30. Pandey BP, Roh C, Choi KY, Lee N, Kim EJ, Ko S, *et al.* 2010. Regioselective hydroxylation of daidzein using P450 (CYP105D7) from *Streptomyces avermitilis* MA4680. *Biotechnol. Bioeng.* **105:** 697-704.

31. Li S, Chaulagain MR, Knauff AR, Podust LM, Montgomery J, Sherman DH. 2009. Selective oxidation of carbolide C–H bonds by an engineered macrolide P450 mono-oxygenase. *Proc. Natl. Acad. Sci. USA* **106:** 18463-18468.

32. Zhang W, Liu Y, Yan J, Cao S, Bai F, Yang Y, *et al.* 2014. New reactions and products resulting from alternative interactions between the P450 enzyme and redox partners. *J. Am. Chem. Soc.* **136:** 3640-3646.

33. Bernhardt R, Urlacher VB. 2014. Cytochromes P450 as promising catalysts for biotechnological application: chances and limitations. *Appl. Microbiol. Biotechnol.* **98:** 6185-6203.